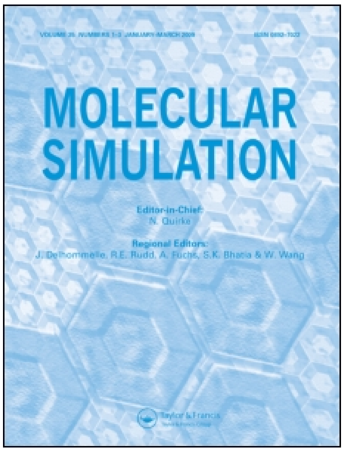

Molecular Simulation
Publication details, including instructions for authors and subscription information:
http://www.informaworld.com/smpp/title~content=t713644482

Effective critical point location: application to thiophenes

J. Pérez-Pellitero[a]; P. Ungerer[b]; A. D. Mackie[a]
[a] Departament d'Enginyeria Química, ETSEQ, Universitat Rovira i Virgili, Av. dels Països Catalans, Tarragona, Spain [b] Institut Français du Pétrole, Rueil Malmaison Cedex, France

To cite this Article Pérez-Pellitero, J. , Ungerer, P. and Mackie, A. D.(2007) 'Effective critical point location: application to thiophenes', Molecular Simulation, 33: 9, 777 — 785

To link to this Article: DOI: 10.1080/08927020701209919

URL: http://dx.doi.org/10.1080/08927020701209919

Molecular Simulation, Vol. 33, Nos. 9–10, 15–30 August 2007, 777–785

Effective critical point location: application to thiophenes

J. PÉREZ-PELLITERO†*, P. UNGERER‡ and A. D. MACKIE†

†Departament d'Enginyeria Química, ETSEQ, Universitat Rovira i Virgili, Av. dels Països Catalans, 26, Campus Sescelades, 43007 Tarragona, Spain
‡Institut Français du Pétrole, 1-4 Av. de Bois Preau, 92852 Rueil Malmaison Cedex, France

(Received December 2006; in final form January 2007)

The anisotropic united atom (AUA) 4 model has been used to calculate the vapor–liquid equilibria of thiophene, 2-methylthiophene and 2,5-dimethylthiophene as well as to locate their critical points using Monte Carlo histogram reweighting (HR) techniques combined with either a fourth order cumulant calculation (Binder parameter) or a mixed-field study. The combination of the cumulant method with the use of finite size scaling is found to present advantages with respect to the mixed-field analysis since no matching to the Ising universal distribution is required while maintaining the same statistical efficiency. In particular, the model critical density of thiophene has been located with a statistical accuracy of less than 0.2% within 3% of the experimental value and the model critical temperature has been located with a statistical accuracy of less than 0.1% within 1% of the experimental value.

Keywords: AUA 4 model; Thiophene; Critical point; Monte Carlo simulation

1. Introduction

The accurate estimation of critical points is important to reproduce thermodynamic data either by using equations of state, other thermodynamic methods or molecular simulation itself. The application of Monte Carlo simulation in principle permits the calculation of the equilibrium properties of any given model fluid. In particular, algorithms such as the Gibbs ensemble (GEMC) greatly simplifies the calculation of the phase equilibria [1]. These methodologies generally have difficulties in accurately estimating the location of critical points due to the appearance of long-range density fluctuations which at the critical point tend to infinity. Instead, finite size scaling (FSS) techniques, originally developed for spin models [2], need to be applied in order to take into account the finite size effects appearing in the neighborhood of the critical point. These techniques provide an efficient way to estimate the infinite system critical parameters from simulations performed at finite size conditions. The FSS methodologies combine in a natural way with histogram reweighting methods (HR). The use of HR enables the calculation of the vapor–liquid equilibrium and critical point location by estimating a density distribution from the information of nearby simulations in an optimal way. In this way, HR is able to rescale the data in order to estimate the system properties as a continuous function of a system parameter such as temperature or chemical potential, which is key to applying FSS efficiently. As has been previously shown [3] for the Lennard–Jones (LJ) pure fluid and mixtures, the combination of the FSS methodologies with the fourth order cumulant calculation, also known as the Binder parameter, allows the critical point to be located in an accurate and straightforward manner. In this work, we extend the application of this methodology to a realistic potential for systems of industrial interest. In particular, the critical point for various members of the family of thiophenes is estimated. The family of thiophenes is of growing importance in the petroleum industry due to the ever-increasing requirements for sulfur removal from fuel. Since the family of thiophenes is much more resistant than thiols or sulfides to existing conversion processes, adsorption [4] is currently being considered as an alternative processes. Hence, there is a strong need for thermodynamic data for these compounds but, unfortunately, there exists only a very limited amount of experimental vapor-equilibrium data in the literature, particularly when dealing with mixtures. To reproduce the equilibrium properties and critical points of this family, we have used the anisotropic united atoms (AUA) 4 model developed by Ungerer *et al.* [5] in which the original AUA

---

*Corresponding author. Email: javier.perez@urv.net

Molecular Simulation
ISSN 0892-7022 print/ISSN 1029-0435 online © 2007 Taylor & Francis
http://www.tandf.co.uk/journals
DOI: 10.1080/08927020701209919

model proposed by Toxvaerd [6,7] has been reparameterized. The AUA model consists of a displacement of the LJ center of force towards the hydrogen atoms, converting the distance of displacement into a third adjustable parameter by contrast with the united atoms (UA) [8] model, where the force centers are placed exactly over the main atom of the UA (usually carbon). Both UA and AUA models results in a significant reduction of computational time as compared to all-atoms models since the number of interacting centers is considerably reduced.

In the present work, we test the aforementioned combination of the location of the universal value of the Binder parameter with FSS methodologies for three compounds of the family of thiophenes: thiophene, 2-methylthiophene and 2,5-dimethylthiophene. We compare our proposed method with standard mixed-field theory where the simulation data needs to be matched to the universal density distribution in order to estimate the finite size critical point. Phase equilibrium properties and normal boiling points have also been calculated for the different compounds. To estimate the phase equilibrium at low temperatures, we propose using the ideal gas assumptions for the vapor phase in order to avoid additional *NPT* simulations, details are given in the section on simulation details.

2. Theory

In this section, a brief overview is given of mixed-field theory, Binder parameter and FSS methodologies used in this work. The HR technique has already been described in a previous work and is based on a method that avoids the explicit construction of histograms [3].

2.1 Mixed-field theory

The FSS technique holds that the coarse-grained properties of systems near the critical point are universal. The concept of universality can be characterized through the probability distribution functions of observables such as density and energy. This is true only for sufficiently large system sizes. For the small values of our simulation box length, L, the properties depend on the specific combination of L and the scaling field measuring the deviation from criticality. For asymmetric models, like the pure LJ fluid, mixed-field theory can be introduced in order to take into account the effects of density and energy fields near the critical point [9,10]. Thus, in the absence of the special symmetry prevailing in the Ising model leading to only one scaling field, the relevant scaling fields will be comprised of linear combinations of the dimensionless temperature and chemical potential difference.

Conjugate to the two relevant scaling fields are scaling operators $\mathcal{M}$ and $\mathcal{E}$, which are comprised of linear combinations of the particle density ρ and energy density u [3]. For models with Ising symmetry, $\mathcal{M}$ is the magnetization while $\mathcal{E}$ is the energy density. The joint distribution of density and energy is simply related to the joint distribution of mixed operators by:

$$P_L(\rho, u) = \frac{1}{1 - sr} P_L(\mathcal{M}, \mathcal{E}) \tag{1}$$

where s and r are system-specific quantities taking into account the contributions of temperature and chemical potential to each of the fields. For pure fluids belonging to the Ising universality class, the critical behavior of the ordering operator distribution $\mathcal{M}$ assumes a scaling form that matches the universal order parameter distribution $p_m^*(x)$ for the Ising model [11]. This means that at the finite critical point of our system, the distribution of our scaling operator $\mathcal{M}$, previously defined as a linear combination of density and energy, should coincide with the Ising model magnetization distribution. The complete procedure followed to determine the critical point of the finite systems according to this methodology is described in more detail elsewhere [3].

2.2 Binder parameter

The Binder cumulant parameter [12] U_L was calculated for different volume sizes using an equal area construction for both phases in equilibrium and is defined as follows:

$$U_L = \frac{\langle m^4 \rangle}{\langle m^2 \rangle^2} \tag{2}$$

with $m = \phi - \langle \phi \rangle$ being ϕ a suitable order parameter, in our case density. The Binder parameter provides a dimensionless measure of the shape of the order parameter distribution function and is expected to have a universal value $U_L = 1.6035$ at the critical point [13] for the Ising universality class. This means that the infinite system size critical point can be identified as the point where U_L becomes system-size independent, being this point where cumulants from different sizes intersect. This is the first method that we use in order to estimate the infinite size critical point from the Binder parameter. Although this estimate is in principle a direct estimate of the infinite system size critical point, there are corrections to scaling that can be used to scale various intersections from different system sizes with system size which have not been considered here. However, it should be noted that these corrections to scaling will cause the intersections of different system sizes, and hence this estimation of the infinite system size critical point, to be also sensitive to the system size, albeit less so than an estimate taken from just one system size.

In this work, we propose an additional method for estimating the critical point. Due to the order parameter distribution based definition of the Binder parameter, the critical conditions can be determined for different system sizes by locating the temperature at which the system takes on the "universal" Ising value of the system. Once these values are calculated, the critical constants are expected to change as a function of the system size according to known scaling laws [10] detailed in the next section. In the Results section, we will present both methods for estimating the infinite system size critical point from the Binder parameter. That is, either by locating the intersection for several system sizes, or as a FSS extrapolation of the estimates for the finite critical temperature taken from the intersection with the Ising universal value.

2.3 Finite size scaling

FSS techniques are applied to determine the thermodynamic limit critical point once the predictions for the apparent critical points have been calculated at different system sizes either by using the mixed-field theory or the "universal" Ising value of the Binder parameters. These apparent critical constants are expected to follow known scaling laws [10].

The temperature of the finite system is expected to vary near the critical point with system size as:

$$\langle T\rangle_c(L) - \langle T\rangle_c(\infty) \sim L^{-(\theta+1)/\nu} \tag{3}$$

where $\Theta = 0.54$ and $\nu = 0.629$ [14,15].

In the case of the critical density of the finite system, it is expected to vary near the critical point with system size as:

$$\langle \rho\rangle_c(L) - \langle \rho\rangle_c(\infty) \sim L^{-(d-1/\nu)} \tag{4}$$

where d is the dimensionality of the system. Additional expressions can be derived for pressure or composition in the case of binary mixtures [16].

Finally, we can estimate the infinite system size value by plotting these system size dependent critical values as is shown in the Results section

3. Model

To describe the dispersion interactions, the different molecules are represented by a set of interacting LJ sites for each CH_3, CH_2, C or S group. The interaction between two different UAs, i and j, from different molecules is calculated according to:

$$U^{\mathrm{LJ}}(r_{ij}) = 4\epsilon_{ij}\left[\left(\frac{\sigma_{ij}}{r_{ij}}\right)^{12}\left(\frac{\sigma_{ij}}{r_{ij}}\right)^{6}\right] \tag{5}$$

To calculate the parameters between unlike UAs, we use the Lorentz–Berthelot combining rules:

$$\epsilon_{ij} = \sqrt{\epsilon_{ii}\epsilon_{jj}} \tag{6}$$

$$\sigma_{ij} = \frac{\sigma_{ii} + \sigma_{jj}}{2} \tag{7}$$

To model the aromatic rings, we have taken the AUA 4 CH intermolecular potential for polyaromatic compounds given by Contreras *et al.* [17], the aromatic C group by Ahunbay *et al.* [18] the methylene group from Ungerer *et al.* [5] and the S group by Pérez *et al.* [19]. The parameters for the different potentials are shown in table 1. In table 2, we show the bond angles and distances used for the different bonds. These parameters have been taken from the experimental geometry of thiophene [20] as well as from *ab initio* calculations. All the models have been assumed to be rigid, as for the AUA 4 model for aromatics. Due to the moderate dipolar moment of the thiophene molecule, $\mu = 0.54D$ [21], we have considered that a simple model without charges should be able to reproduce accurately the vapor–liquid equilibrium properties, at least of pure systems.

Table 1. LJ parameters.

Group	*σ (Å)*	*ϵ/k (K)*	*δ (Å)*
CH_3 [5]	3.607	120.15	0.216
CH [17]	3.246	89.42	0.407
C [18]	3.246	37.73	–
S	3.493	179.2	–

4. Simulation details

The equilibrium properties and critical points of the different compounds considered were obtained using grand canonical Monte Carlo (GCMC) simulations combined with HR [22,23]. An additional bias for the insertion of the first center of the molecules [25] as implemented to enhance the rate of insertions. The probabilities of the different moves used in the simulations were 0.15 for translation, 0.15 for rotation and 0.7 for insertion or deletion. A simulation box of size $L = 32$ Å was used in all cases. Additional simulations in the critical region were done for the different molecules using system sizes ranging from $L = 25$ up to 42 Å.

In previous works [5], the phase coexistence densities were calculated by using additional simulations in the isothermal isobaric (*NPT*) together with the Clapeyron equation. In this work, we use the same approximations used in the previous works but use HR along with simulations carried out in the grand canonical ensemble. In particular, due to the limited number of particles present in the box for the vapor phase at low temperatures, we have calculated the enthalpy according to:

$$\Delta H_{\mathrm{vap}} = -\langle E_{\mathrm{liq(inter)}}\rangle + RT \tag{8}$$

where $\langle E_{\mathrm{liq(inter)}}\rangle$ is the average molar intermolecular potential energy in the simulation. This expression assumes that (i) the molar volume of the liquid is negligible

Table 2. Bond lengths and angles.

Bond	*Length (Å)*	*Angle*	*Σ(deg)*
C—C	1.53	C—C—C	112.7
C—C (aromatic ring)	1.39	C—S—C	92.2
C—S	1.72	C—C—S	111.2

compared with that of the vapor, (ii) the vapor is close enough to an ideal gas and (iii) the difference between the intramolecular energies of the two phases is negligible. These assumptions are indeed justified for reduced temperatures T/T_c lower than 0.6, which corresponds to vapor pressures significantly lower than atmospheric pressure.

In this way, the enthalpy can be calculated reliably, since the molar volume of the gas is estimated through the ideal gas law, not being affected by the error committed due to the low number of molecules in the vapor phase. Then the pressure at such low temperatures can be determined by integrating the Clapeyron equation using the enthalpies calculated by means of equation (8)

$$\left(\frac{\mathrm{d}\ln P_{\mathrm{sat}}}{\mathrm{d}(1/T)}\right) = -\frac{\Delta H_{\mathrm{vap}}}{R} \tag{9}$$

The integration can be done by using a second order scheme with regularly spaced $1/T$ values:

$$\ln P_{\mathrm{sat}}^{(n+1)} = \ln P_{\mathrm{sat}}^{(n-1)} - \frac{\Delta H_{\mathrm{vap}}^{n}}{R}\left[\frac{1}{T^{(n+1)}} - \frac{1}{T^{(n-1)}}\right] \tag{10}$$

Finally, we have checked this methodology by comparing the results with additional *NPT* simulations in order to ensure that the energy and density of the liquid phase are not affected by these approximations, as will be shown in the results section.

5. Results

The vapor–liquid coexistence curves for three alkylthiophenes (thiophene, 2-methylthiophene and 2,5-dimethylthiophene) have been calculated using the AUA 4 model. The results for the vapor–liquid phase coexistence densities are shown in figure 1. In figure 2, we show the liquid vapor results for thiophene in more detail, also given are the results obtained by Lubna *et al.* [26] for their UA model. As can be seen in the inset, results of additional *NPT* simulations at low temperatures are also shown in order to validate the method described in Section 4. Below a temperature of 0.65 T_c, the results shown from HR are estimated by applying this method. There is an excellent agreement for the coexistence liquid densities between both methodologies. This agreement confirms that the proposed method is consistent with the *NpT* simulations.

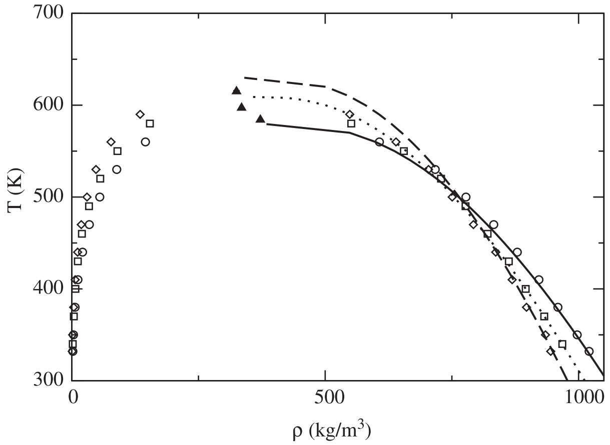

Figure 1. Coexistence curves of alkylthiophenes. Solid, dashed and dotted lines represent experimental data [21] for thiophene, 2-methylthiophene and 2,5-dimethylthiophene respectively. Circle, square, and diamond symbols represent the simulation results for thiophene, 2-methylthiophene and 2,5-dimethylthiophene, respectively. Filled triangles denote estimates of the critical points of this model.

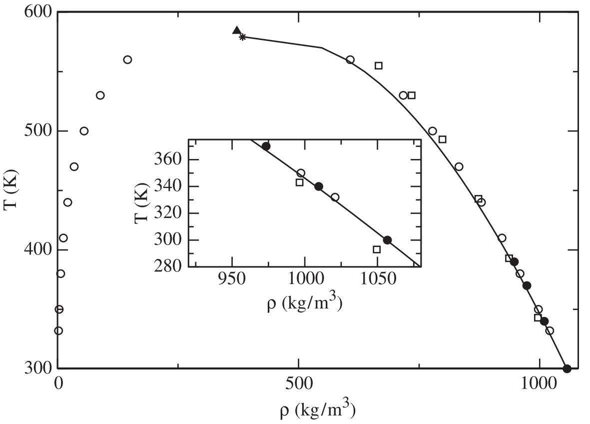

Figure 2. Coexistence curve of thiophene. The solid line represents experimental data [21], open circles are the HR results of the new model. Squares are GEMC simulation results of the TRAPPE model from Ref. [26]. The triangle represents the critical point of this model. Filled symbols represent *NPT* simulations results.

Three different techniques have been used to locate the critical point of the different compounds. In the first place, we have used the conventional matching to the universal order parameter distribution by using mixed-field theory. In figure 3, we show the results obtained for this matching in the case of thiophene using a system size of $L = 37$ Å. The scaling factor a_L and the scaling index β/ν have been chosen so that the scaling variable x has unit variance [27].

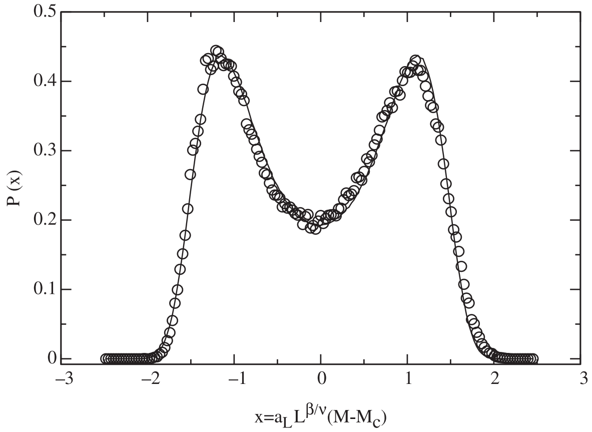

Figure 3. Ordering operator distribution at the apparent critical conditions as a function of the scaling variable $x \equiv a_L L^{\beta/\nu}(\mathcal{M} - \mathcal{M}_c)$. The solid line represents the fixed point $p_m^*(x)$ for the Ising universality class [11] while the circles represents simulation results for thiophene at $L^* = 37$ Å.

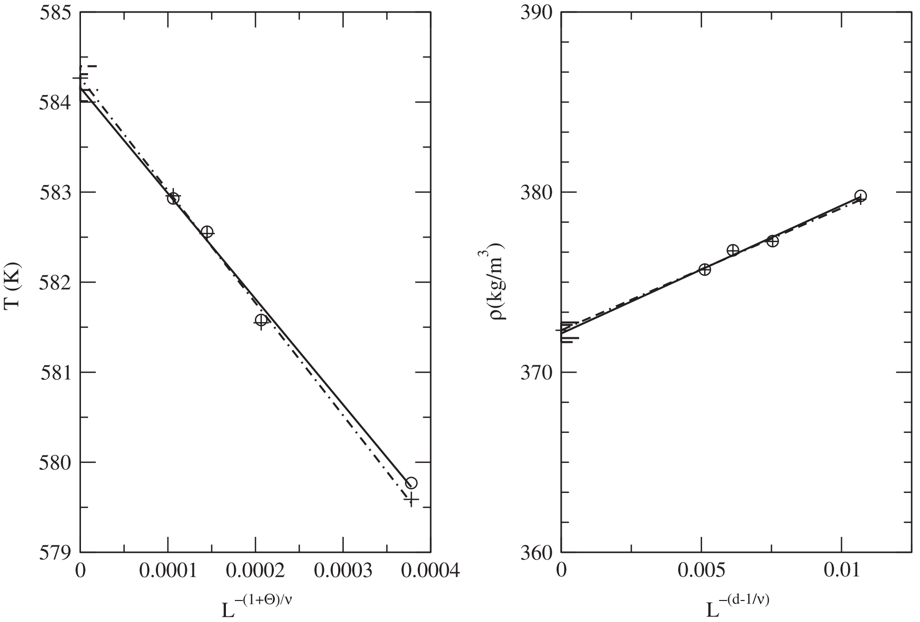

Figure 4. Thiophene apparent critical temperature $T_c^*(L)$ expressed as a function of $L^{-(\Theta+1)/\nu}$ and apparent critical density $\rho_c^*(L)$ expressed as a function of $L^{-(d-1/\nu)}$ Crosses are mixed-field results, empty circles are cumulant results. Dot-dashed lines represent least-squares fits of the mixed-field data, solid lines represent least-squares fits of the Binder parameter data.

A good agreement is found between the simulation results of this work and the literature Ising values [11]. After repeating this procedure for the different system sizes, we have applied equations (9)–(10) to extrapolate to infinite volume in order to obtain the thermodynamic limit critical point. In figures 4–6, the results of this scaling for the three different molecules are given. We have obtained, in general, an excellent agreement for both temperature and density with the expected linear tendency, confirming the validity of the scaling laws in the studied range of system sizes. In the second place, as can be seen in figures 7–9 for the different molecules, we have determined the critical points by using the intersections of the Binder parameter calculated along the equilibrium line for the different system sizes considered. As can be seen, the intersections take place close to the universal Ising value of the Binder parameter $U_L = 1.6035$ [13]. This fact can be taken as a universality class mark, as in the case of the mixed-field theory for the matching condition to the universal order parameter distribution, indicating that these systems most

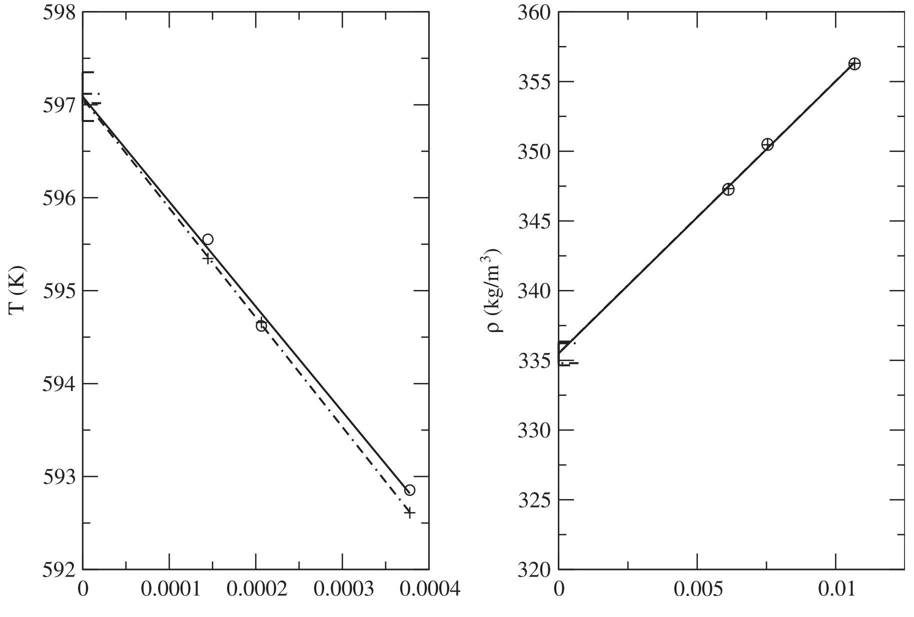

Figure 5. 2-Methylthiophene apparent critical temperature $T_c^*(L)$ expressed as a function of $L^{-(\Theta+1)/\nu}$ and apparent critical density $\rho_c^*(L)$ expressed as a function of $L^{-(d-1/\nu)}$ Crosses are mixed-field results, empty circles are cumulant results. Dot-dashed lines represent least-squares fits of the mixed-field data, solid lines represent least-squares fits of the Binder parameter data.

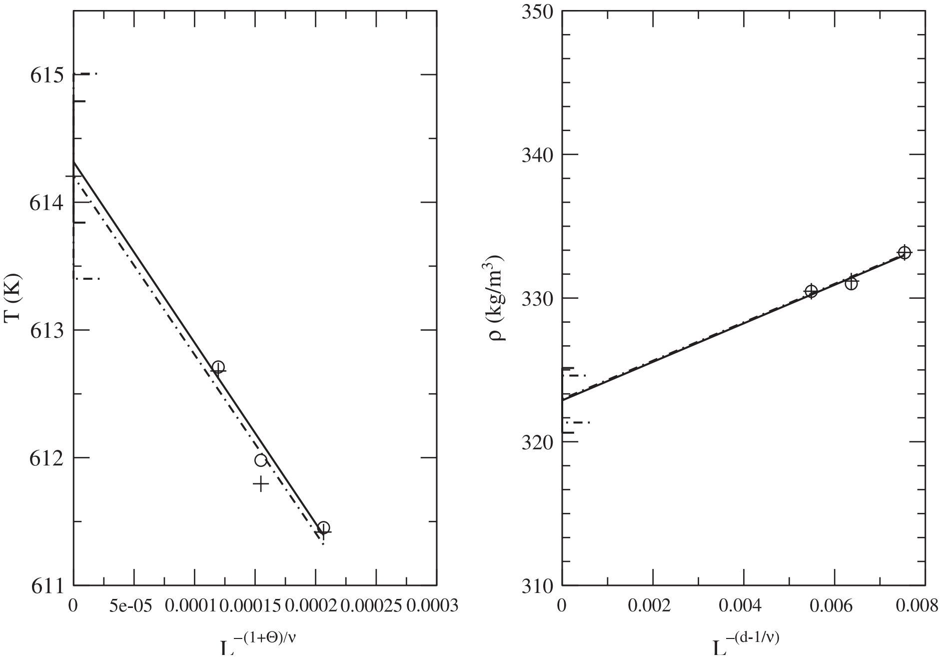

Figure 6. 2,5-Dimethylthiophene apparent critical temperature $T_c^*(L)$ expressed as a function of $L^{-(\Theta+1)/\nu}$ and apparent critical density $\rho_c^*(L)$ expressed as a function of $L^{-(d-1/\nu)}$ Crosses are mixed-field results, empty circles are cumulant results. Dot-dashed lines represent least-squares fits of the mixed-field data, solid lines represent least-squares fits of the Binder parameter data.

likely belong to the Ising universality class as expected. Furthermore, at least in the case of thiophene, it seems that the intersections approach the universal value of the Binder parameter as the size of the system is increased. This fact is attributed to the correction terms present in the formulation of U_L when the size is too small [28]. As a consequence, the value of U_L is slightly shifted from the universal value obtained for the Ising model and hence the predicted critical temperatures are slightly overestimated as compared to the FSS methodologies results. Finally, as described in Section 2 and taking into account that the Binder parameter provides a dimensionless measure of the order parameter distribution, we have taken the intersections of the Binder parameter with its universal "Ising" value in order to obtain in a straightforward way estimations for the system-size dependent critical points, see insets in figures 7–9. As mentioned before, and also shown in figures 4–6, these estimates can be extrapolated to infinite volume to recover the critical point in the thermodynamic limit. As in the case of the mixed-field theory, we have obtained again the expected linear tendency according to the scaling laws. In table 3, we

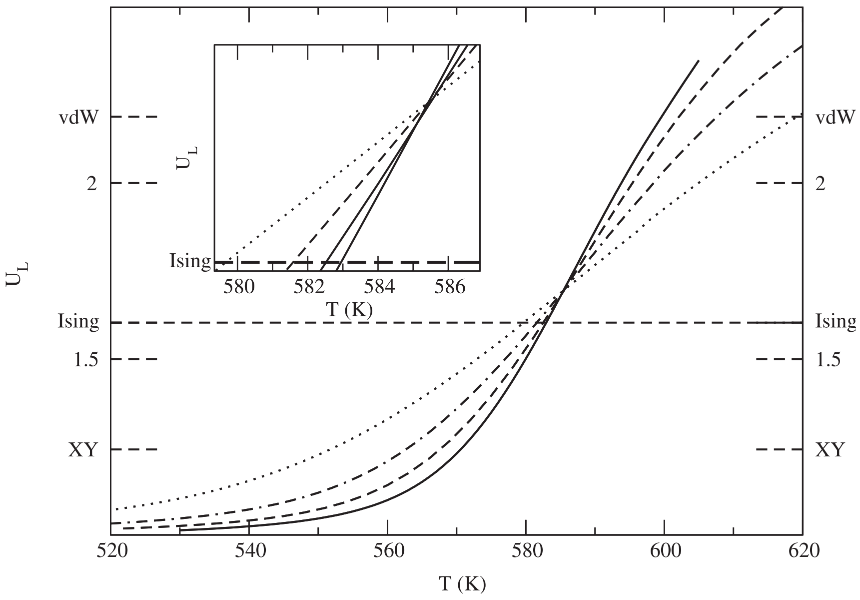

Figure 7. Binder parameter intersections for different system sizes for thiophene. Classical, XY and Ising values of U_L are shown [13].

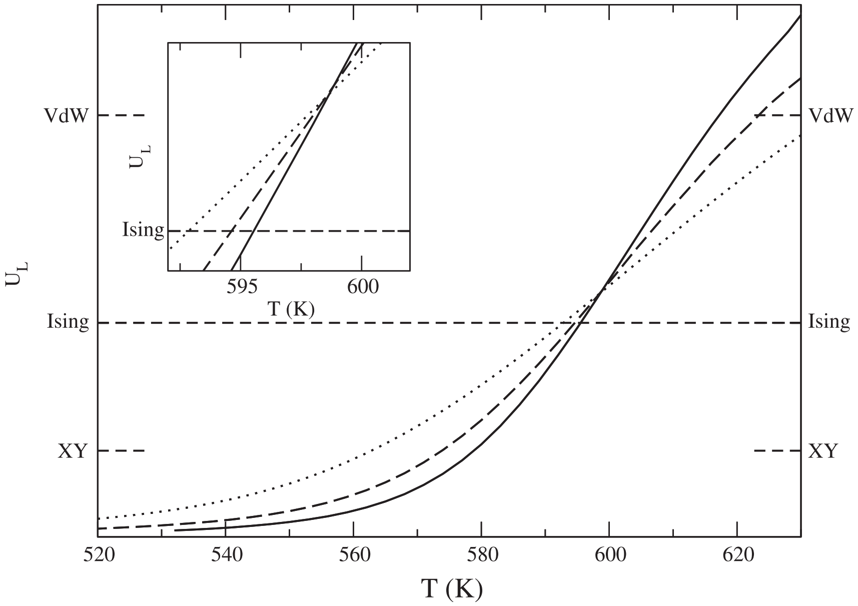

Figure 8. Binder parameter intersections for different system sizes for 2-methylthiophene. Classical, XY and Ising values of U_L are shown [13].

present the results obtained as a function of the applied methodology as well as the experimental data of Ref. [21]. The results obtained for the different applied methodologies are in good agreement between themselves. In particular, both the FSS techniques give a similar statistical precision, which is higher than that for the cumulant intersecton method. These errors are within 0.1% for the critical temperature and 0.2% for the critical density for FSS and about 0.3% and 0.4% for respectively for the cumulant intersection. In the case of Gibbs ensemble calculations, where the coexistence densities are extrapolated to the critical point using the appropriate scaling law as well as the law of rectilinear diameters, typical statistical errors are significantly higher at approximately 0.5 and 1.5%, respectively for the critical temperature and density [26,29]. With respect to the experimental value of the critical point, we find our model value to be within 1% for thiophene, about 2% in the case 2-methylthiophene and 2.5% for 2,5-dimethylthiophene for the critical temperature and 3%, 6% and 6%, respectively for the critical density.

6. Conclusions

The AUA 4 model has been used to obtain phase equilibrium data of the family of thiophenes. Despite the simplicity of the model, no charges have been introduced

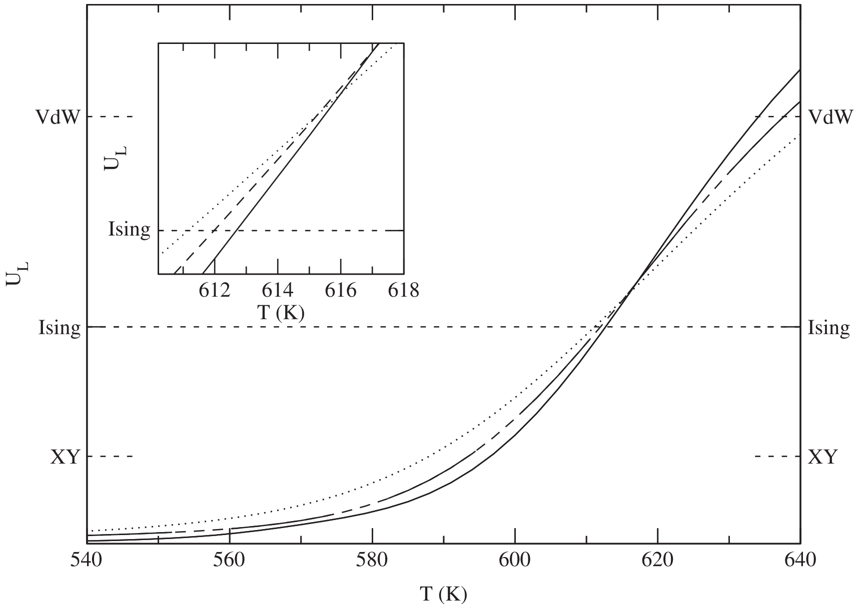

Figure 9. Binder parameter intersections for different system sizes for 2,5-dimethylthiophene. Classical, XY and Ising values of U_L are shown [13].

Table 3. Critical properties of the different compounds.

Molecule	*Molecule*	*Type*	$T_c(K)$	$\rho_c(kg/m^3)$
Thiophene	Thiophene	Mixed-field theory + FSS	584.2(2)	372.6(4)
		Cumulant + FSS	584.1(2)	372.1(4)
		Cumulant intersection	585(1)	377(2)
		Experiment	579	384
2-Methylthiophene	2-Methylthiophene	Mixed-field theory + FSS	597.1(1)	335.5(7)
		Cumulant + FSS	597.1(3)	335.5(8)
		Cumulant intersection	598(1)	335(1)
		Experiment	609	357
2,5-Dimethylthiophene	2,5-Dimethylthiophene	Mixed-field theory + FSS	614.2(8)	323(2)
		Cumulant + FSS	614.3(5)	323(2)
		Cumulant intersection	615(3)	325(5)
		Experiment	630	342

and a rigid geometry is considered, very good agreement has been obtained for the different properties. In particular, the critical temperature has been reproduced to within 1% in the case of thiophene, 2% for 2-methylthiophene and 2.5% for 2,5-dimethylthiophene. To determine the critical parameters, we have applied three different techniques: the fourth order cumulant or Binder parameter intersection method, the Binder parameter intersection with the universal value with FSS and mixed-field theory with FSS. The main advantage of the Binder parameter with universal value method compared with the mixed-field theory is that no matching of the Ising universal distribution is required making the estimation of the finite critical point more straightforward. We find excellent agreement between the results obtained with all three methods and equal statistical performance for the two FSS methods.

To summarize, we have shown that for realistic intermolecular potentials, the combination of HR techniques with the Binder fourth order cumulant calculation is completely equivalent to the mixed-field method and can be employed in a FSS study in order to estimate the critical parameters with the same precision as for the mixed-field studies.

Acknowledgements

This study was supported by the Spanish Government, *Ministerio de Educación y Ciencia* (Grant No. CTQ2004-03346/PPQ) as well as the *Institut Français du Pétrole.* The simulations have been carried out using the GIBBS Monte Carlo code developed jointly by the *Institut Français du Pétrole.*, *Université de Paris Sud, CNRS* and other partners.

References

[1] A.Z. Panagiotopoulos. Direct determination of phase coexistence properties of fluids by Monte-Carlo simulation in a new ensemble. *Mol. Phys.*, **61**, 813 (1987).

[2] U. Wolff. *Computational Methods in Field Theory*, Springer, (1992).

[3] J. Pérez-Pellitero, P. Ungerer, G. Orkoulas, A.D. Mackie. Critical point estimation of the Lennard-Jones pure fluid and binary mixtures. *J. Chem. Phys.*, **125**, 054515 (2006).

[4] C.O. Ania, T.J. Bandosz. Sodium on the surface of activated carbons as a factor enhancing reactive adsorption of dibenzothiophene. *Energy Fuels*, **20**, 1076 (2006).

[5] P. Ungerer, C. Beauvais, J. Delhommelle, A. Boutin, B. Rousseau, A.H. Fuchs. Optimization of the anisotropic united atoms intermolecular potential for n-alkanes. *J. Chem. Phys.*, **112**, 5499 (2000).

[6] S. Toxvaerd. Equation of state of alkanes. 2. *J. Chem. Phys.*, **107**, 5197 Bias (1997).

[7] S. Toxvaerd. Molecular-dynamics calculation of the equation of state of alkanes. *J. Chem. Phys.*, **107**, 4290 (1990).

[8] M.G. Martin, J.I. Siepmann. Transferable potentials for phase equilibria. 1. United-atom description of n-alkanes. *J. Phys. Chem. B*, **102**, 2569 (1998).

[9] N.B. Wilding, A.D. Bruce. Density-fluctuations and field mixing in the critical fluid. *J. Phys. Condensed Matter*, **4**, 3087 (1992).

[10] N.B. Wilding. Critical-point and coexistence-curve properties of the Lennard-Jones fluid - a finite-size-scaling study. *Phys. Rev. E*, **52**, 602 (1995).

[11] Data for the "universal operator distribution" Private communication N. Wilding.

[12] K. Binder. Finite size scaling analysis of Ising-model block distribution-functions. *Z. Phys. B Condensed Matter*, **43**, 119 (1981).

[13] E. Luijten, M.E. Fisher, A.Z. Panagiotopoulos. Universality class of criticality in the restricted primitive model electrolyte. *Phys. Rev. Lett.*, **88**, 185701 (2002).

[14] A.M. Ferrenberg, D.P. Landau. Critical-behavior of the 3-dimensional Ising-model – a high-resolution Monte-Carlo study. *Phys. Rev. B*, **44**, 5081 (1991).

[15] J.H. Chen, M.E. Fisher, B.G. Nickel. Unbiased estimation of corrections to scaling by partial-differential approximants. *Phys. Rev. Lett.*, **48**, 630 (1982).

[16] J.J. Potoff, A.Z. Panagiotopoulos. Critical point and phase behavior of the pure fluid and a Lennard-Jones mixture. *J. Chem. Phys.*, **109**, 10914 (1998).

[17] R.O. Contreras-Camacho, P. Ungerer, M.G. Ahunbay, V. Lachet, J. Pérez-Pellitero, A.D. Mackie. Optimized intermolecular potential for aromatic hydrocarbons based on anisotropic united atoms. 2. Alkylbenzenes and styrene. *J. Phys. Chem. B*, **108**, 14115 (2004).

[18] M.G. Ahunbay, J. Pérez-Pellitero, R.O. Contreras-Camacho, J.M. Teuler, P. Ungerer, A.D. Mackie, V. Lachet. Optimized intermolecular potential for aromatic hydrocarbons based on anisotropic united atoms. III. Polyaromatic and naphthenoaromatic hydrocarbons. *J. Phys. Chem. B*, **109**, 2970 (2005).

[19] J. Pérez-Pellitero, P. Ungerer, A.D. Mackie. *J. Phys. Chem. B*. (In press 2007) .

[20] Handbook of Chemistry and Physics, CRC Press, (1993).

[21] BYU DIPPR 801, *Thermophysical Properties Database Public Release January 2005*.

[22] A.M. Ferrenberg, R. Swendsen. New Monte-Carlo technique for studying phase-transitions. *Phys. Rev. Lett.*, **61**, 2635 (1988).

[23] A.M. Ferrenberg, R. Swendsen. Optimized Monte-Carlo data-analysis. *Phys. Rev. Lett.*, **63**, 1195 (1989).

[24] E. Bourasseau, P. Ungerer, A. Boutin. Prediction of equilibrium properties of cyclic alkanes by Monte Carlo simulation – new anisotropic united atoms intermolecular potential – New transfer bias method. *J. Phys. Chem. B*, **106**, 5483 (2002).

[25] A.D. Mackie, B. Tavitian, A. Boutin, A.H. Fuchs. Vapour-liquid phase equilibria predictions of methane-alkane mixtures by Monte Carlo simulation. *Mol. Simul.*, **19**, 1 (1997).

[26] N. Lubna, G. Kamath, J.J. Potoff, N. Rai, J.I. Siepmann. Transferable potentials for phase equilibria. 8. United-atom description for thiols, sulfides, disulfides, and thiophene. *J. Phys. Chem. B*, **109**, 24100 (2005).

[27] W. Shi, J. Johnson. Histogram reweighting and finite-size scaling study of the Lennard-Jones fluids. *Fluid Phase Equilib.*, **187**, 171 (2001).

[28] D.P. Landau, K. Binder. *Monte Carlo Simulations in Statistical Physics*, Cambridge University Press, (2000).

[29] B. Chen, J.J. Potoff, J. Siepmann. Monte Carlo calculations for alcohols and their mixtures with alkanes. Transferable potentials for phase equilibria. 5. United-atom description of primary, secondary, and tertiary alcohols. *J. Phys. Chem. B*, **105**, 3093 (2001).